JOURNAL OF SPACECRAFT AND ROCKETS
Vol. 46, No. 2, March–April 2009

Investigations into Synergistic Effects of Atomic Oxygen and Vacuum Ultraviolet

Hiroyuki Shimamura* and Eiji Miyazaki*
Japan Aerospace Exploration Agency, Tsukuba, Ibaraki 305-8505, Japan

DOI: 10.2514/1.31815

Polymer materials exposed to a space environment exhibit strongly degraded properties because of environmental factors, for example, atomic oxygen, vacuum ultraviolet, and radiation. In addition, the degradation of polymer materials can be accelerated because of the synergistic effects of these environmental factors. For designing high-reliability spacecraft, it is important to understand precisely the polymer materials' degradation. In this report, the synergistic effects of atomic oxygen and vacuum ultraviolet on polyimide films, Kapton H, and silver-coated fluorinated ethylene propylene films were investigated through comparison of the degradation behaviors after single, sequential, and simultaneous irradiations. For both materials, there was no significant change attributed to the synergistic effects in erosion yield and thermo-optical properties. However, the surface morphology of silver-coated fluorinated ethylene propylene changed substantially depending on the irradiation method. Surfaces of silver-coated fluorinated ethylene propylene were eroded by atomic oxygen, but were smoothed by vacuum ultraviolet. The surface morphology after sequential irradiations differed depending on the irradiation sequence. A rougher surface with low blunt cones was produced after simultaneous irradiation because of the interaction of the erosion by atomic oxygen attacks and smoothing by vacuum ultraviolet irradiation. This report also describes the measurement methods for fluence of each beam under simultaneous irradiation.

Nomenclature

A_m	=	exposure area of the atomic oxygen fluence monitor, Kapton H, 3.14 cm^2
A_s	=	exposure area of samples
E_m	=	erosion yield of the atomic oxygen fluence monitor, Kapton H, 3×10^{-24} cm^3/atom
E_s	=	erosion yield of samples
F	=	atomic oxygen fluence
F_{sim}	=	atomic oxygen fluence under simultaneous irradiation
X	=	distance form the outer edge of the sample holder
Δm_{msh}	=	mass loss of the atomic oxygen fluence monitor, Kapton H, placed on the sample holder
Δm_{mlvp}	=	mass loss of the atomic oxygen fluence monitor, Kapton H, placed on the little vacuum-ultraviolet-influenced position
Δm_s	=	mass loss of samples
Δt_s	=	thickness loss of samples
ρ_m	=	density of the atomic oxygen fluence monitor, Kapton H, 1.42 g/cm^3
ρ_s	=	density of samples

I. Introduction

THE space environment includes numerous destructive environmental factors such as atomic oxygen (AO), ultraviolet (UV), various types of radiations, thermal cycling, meteoroids, and space debris. Polymer materials used in spacecraft are usually damaged both chemically and physically by these environmental factors. Major environmental factors related to the degradation of polymer materials' properties are AO, UV, and radiation. Especially in a low Earth orbit (LEO), materials that are exposed directly to a space environment collide with AO at high velocity: about 8 km/s. The exposed polymer materials are eroded and lose their weight through such AO attacks, developing a light-diffusing *needlelike* surface [1]. This change of the surface texture might decrease the optical reflectance and increase solar absorptance. Moreover, AO attacks degrade polymers' mechanical properties [2]. Crack initiations can be produced easily on the needlelike surface. These degradations might cause a significant failure of spacecraft systems: its thermal, optical, or structural design. Therefore, ground simulation tests are mandatory techniques for space programs in terms of the degradation assessment of space polymer materials.

In ground simulation tests, single, sequential, and simultaneous irradiation tests using AO, UV, and radiation sources have been carried out to simulate the space environmental degradation of polymer materials [3–5]. For some materials, synergistic degradation phenomena are observed only by simultaneous irradiation. For instance, in a polyimide film, when vacuum ultraviolet (VUV) irradiation is added to AO, the AO erosion is accelerated, resulting in higher mass loss than the value predicted from AO fluence [6,7]. Therefore, the degradation of polymer materials is needed to be assessed by the simultaneous irradiation.

In this report, the synergistic effects of AO and VUV on polyimide films, Kapton H, and silver-coated fluorinated ethylene propylene (Ag-coated FEP) films, which are commonly used for space, are investigated through comparison of the degradation behaviors after single, sequential, and simultaneous irradiations. All irradiation tests were performed using the Combined Space Effects Test Facility in Tsukuba Space Center, Japan Aerospace Exploration Agency (JAXA) [8]. It is important to take an accurate measurement of AO and VUV fluence to simulate a certain orbital environment via simultaneous irradiation. However, it is difficult to measure accurately the AO and VUV fluence under simultaneous irradiation with the standard methods for the facility, because each beam affects the detector for the other beam. The measurement methods to determine the AO and VUV fluence under simultaneous irradiation are also discussed in this report.

II. Experimental

A. Combined Space Effects Test Facility

1. Specifications and Configurations

Equipped with AO, VUV, and electron beams (EB) sources, the Combined Space Effects Test Facility can irradiate these beams simultaneously into an irradiation chamber with a high vacuum of

Received 27 June 2007; accepted for publication 25 June 2008. Copyright © 2008 by the American Institute of Aeronautics and Astronautics, Inc. All rights reserved. Copies of this paper may be made for personal or internal use, on condition that the copier pay the $10.00 per-copy fee to the Copyright Clearance Center, Inc., 222 Rosewood Drive, Danvers, MA 01923; include the code 0022-4650/09 $10.00 in correspondence with the CCC.

*Engineer, Space Materials Section, Advanced Materials Group, Aerospace Research and Development Directorate, 2-1-1 Sengen.

Table 1 Standard specifications of the Combined Space Effects Test Facility

Item	Value
Vacuum	10^{-5} Pa (10^{-3}–10^{-2} Pa during AO irradiation)
Sample	Size: 25 mm diam × max 3 mm thick
	Exposure area: 20 mm diam
	Quantity: 16 samples per holder
AO	Method: laser detonation
	Laser: pulsed CO_2 laser
	Laser wavelength: 10.6 μm
	Pulse rate: 12 Hz
	Laser output power: ~10 J/pulse
	Beam velocity: 8 km/s
	Translational energy: 5 eV
	Flux: $\sim 5 \times 10^{15}$ atoms/cm$^2 \cdot$ s
VUV	Source: 30 W deuterium lamps
	Number of lamps: 48
	Lamp current: 250–350 mA
	Tube voltage: 70–90 V
	Flux: 0.3–0.5 mW/cm^2
	(Integral intensity at a wavelength of 120–200 nm)
EB	Accelerating voltage: 100–500 kV
	Source current: 0.1–2.0 mA
Sample temperature	−150–80 °C

about 10^{-5} Pa. Standard specifications of the facility are listed in Table 1; its schematic view is shown in Fig. 1. The linear motion feedthrough is installed in the irradiation chamber, which is located over the sample holder and which can move parallel to the sample holder's plane. A photodiode or a quartz crystal microbalance (QCM) can be attached on the linear motion feedthrough.

The AO generation in the facility is based on the laser detonation phenomenon invented by Physical Science, Inc. The AO beam source is composed of the pulsed valve and the pulsed CO_2 laser at a wavelength of 10.6 μm with a pulse energy of about 10 J. The translational energy of the hyperthermal AO produced by the facility is controlled at approximately 5 eV to replicate the LEO environment.

The VUV sources, a total of 48 deuterium lamps (L2581; Hamamatsu Photonics K.K.), are installed in the lamp chamber, which had been purged using high-purity Ar gas. The VUV beam from the lamps is concentrated by the CaF_2 lens and collection mirror coated with Al and MgF_2; it is then injected into the irradiation chamber through an MgF_2 plate separating the lamp chamber and the irradiation chamber.

2. Standard Methods for Atomic Oxygen and Vacuum Ultraviolet Fluence Measurements

A polyimide film, Kapton H, mounted on the sample holder is used as an AO fluence monitor because of the fact that its known mass loss is proportional to the irradiated AO fluence [1]. The AO fluence is calculated from the mass loss of the AO fluence monitor on the sample holder through Eq. (1):

$$F = \Delta m_{\mathrm{msh}} / A_m \rho_m E_m \tag{1}$$

The VUV irradiated on the samples is attenuated in its light path. The spectrum of the VUV irradiated on the samples is estimated from the original lamp spectrum [9] by considering these attenuations and by calibrating with the VUV intensity on the sample holder at a wavelength of 150–170 nm, which is measured using the photodiode attached on the linear motion feedthrough placed over the sample holder. Then, the integral intensity of VUV at a wavelength of 120–200 nm is calculable from the estimated VUV spectrum.

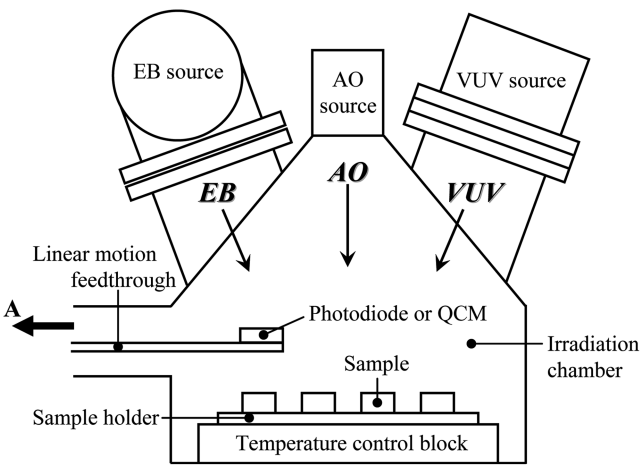

Fig. 1 Schematic view of the Combined Space Effect Test Facility.

B. Procedures for Establishment of Beam Fluence Measurements Under Simultaneous Irradiation

1. Atomic Oxygen Fluence Measurement Under Simultaneous Irradiation

The AO fluence monitor, Kapton H, mounted on the sample holder is exposed to AO and VUV during simultaneous irradiation. It is noteworthy that the mass loss rate is accelerated by additional VUV irradiation, as described before. Therefore, Kapton H on the sample holder is not available for an AO fluence monitor under simultaneous irradiation. It is necessary to find a position that is sufficiently irradiated by AO and which is little irradiated by VUV. The AO fluence under simultaneous irradiation should be calculated from the mass loss of the AO fluence monitor placed on such position.

First, the VUV-influenced area was distinguished using a photodiode attached on the linear motion feedthrough. The photodiode started measurements of VUV intensity at the position just over the outer edge of the sample holder; then, it was moved gradually to the direction denoted as A in Fig. 1 while monitoring the intensity. Secondly, to investigate whether AO can irradiate the position where the VUV intensity is quite small, called the "little VUV-influenced position," the mass change of polyimide placed in this position was evaluated during AO irradiation. The mass change of polyimide was monitored using the QCM with gold electrodes attached on the linear motion feedthrough. The sensor crystals were coated with polyimide varnish (U-varnish; Ube Industries, Ltd.). As the mass of the polyimide coating on the sensor crystal decreases by AO irradiation, the frequency of the QCM increases. As a result, the mass change is visible in situ. Then, VUV irradiation was added to AO to confirm whether VUV affects the mass change of polyimide at the little VUV-influenced position or not. Finally, the AO fluence monitor, Kapton H, was set on the sample holder and the little VUV-influenced position. The mass losses of Kapton H on both positions were compared after AO irradiation to estimate the AO fluence on the sample holder from the mass loss of Kapton H placed on the little VUV-influenced position.

2. Vacuum Ultraviolet Fluence Measurement Under Simultaneous Irradiation

In simultaneous irradiation of AO and VUV, a photodiode detects the total intensity of the VUV from the sources and from by-products emitted in the AO generation process [10]. It is necessary to eliminate the VUV emitted in AO generation from the total intensity to determine the targeted VUV fluence, that is, VUV from the sources, under simultaneous irradiation.

The VUV intensity during single AO or VUV irradiation, and simultaneous irradiation of AO and VUV, were measured using a photodiode attached on the linear motion feedthrough, which was placed over the sample holder. The photodiode was covered with a MgF_2 plate (Nakajima Giken Co., Ltd.), which is known to have a high transmittance at the VUV wavelength region, to protect its sensing element from AO attacks.

Table 2 AO and VUV fluence in irradiation tests

Irradiation method		AO fluence, 10^{20} atoms/cm^2	VUV fluence, 10^4 mJ/cm^2 (at 120–200 nm)
Single	AO	1.9–2.3	——
	VUV	——	1.1
Sequential	AO → VUV	1.9–2.3	1.1
	VUV → AO	1.9–2.3	1.1
Simultaneous	AO + VUV	2.7–3.0	1.1

C. Evaluation of the Synergistic Effects of Atomic Oxygen and Vacuum Ultraviolet

1. Materials

The polyimide films (25-μm thickness, Kapton H; DuPont) and the Ag-coated (one side) FEP films (25-μm thickness; Sheldahl) were used as tested samples. The 25-mm-diam samples were cut from a sheet using a punch to fit the irradiation facility's sample holder. For Ag-coated FEP, the FEP surface side was exposed.

2. Single, Sequential, and Simultaneous Irradiations

Single, sequential, and simultaneous irradiation tests were conducted using an AO and/or VUV source. The AO and VUV fluence levels for each irradiation test are shown in Table 2. These fluence levels were equivalent to those in the LEO environment around 400 km altitude for 3 months, according to the analysis using the Space Environment and Effect System (SEES: JAXA's database system for providing data and models related to space environments and effects of space environments). In the simultaneous irradiation test, the AO fluence was greater than that of the other tests because the irradiation time was adjusted to unify the VUV fluence with other irradiation tests. During irradiation tests, the sample surfaces were kept at room temperature.

3. Mass and Erosion Yield Measurements

A microbalance (MX5; Mettler Toledo International, Inc.) was used for mass measurements of samples before and after irradiation tests. For the samples, water absorption into the sample is apparent during weighing. For this reason, it must be compensated by extrapolation of the mass increase curve plotted during weighing of the sample to calculate the dry mass. The weighing procedure is as follows: the sample is first stored in a desiccator for at least 24 h; it is brought onto the microbalance under controlled ambient conditions, $23 \pm 2\,^{\circ}$C and $50 \pm 5\%$ relative humidity; the mass is plotted for 180 s after removal of the sample from the desiccator. That measurement is then fitted to a quadratic curve to obtain the estimated dry mass from the intercept of the fitted curve.

From the mass change during irradiation, the erosion yield was calculated using Eq. (2):

$$E_s = \Delta m_s / A_s \rho_s F \tag{2}$$

where $\rho_s = 1.42$ g/cm^2 for Kapton H, and $\rho_s = 2.15$ g/cm^2 for Ag-coated FEP.

4. Thermo-Optical Properties Evaluation

The thermo-optical properties, solar absorptance α_S, and normal infrared emittance ε_N were measured using a spectrophotometer (U-4100; Hitachi High-Technologies Corp.) and a portable reflectometer (TESA 2000; AZ Technology Corp.) before and after irradiation tests.

5. Surface Morphology Observation

The surface morphology observations for pristine control samples and irradiated samples were conducted using atomic force microscopy (AFM, SPM-9500; Shimadzu Corp.).

III. Results and Discussion

A. Beam Fluence Measurements Under Simultaneous Irradiation

1. Atomic Oxygen Fluence Measurement Under Simultaneous Irradiation

The VUV intensity at a wavelength of 150–170 nm for the distance from the outer edge of the sample holder, symbolized by X, is shown in Fig. 2. In this figure, the position where $X = 0$ cm represents the outer edge of the sample holder. It was indicated that the VUV intensity decreased as the distance from the sample holder increased. The intensity decreased to a few percent of that over the outer edge of the sample holder at $X \geq 14$ cm. Therefore, the position where $X \geq 14$ cm can be regarded as the little VUV-influenced position.

Figure 3 presents the measured frequency of the QCM and the frequency change rate during single AO irradiation and simultaneous irradiation of AO and VUV. The QCM was located at $X \cong 16$ cm, which is in the little VUV-influenced position. Figure 3 shows that the QCM frequency increased because of mass loss in the polyimide coating with continuing AO irradiation. Furthermore, no marked

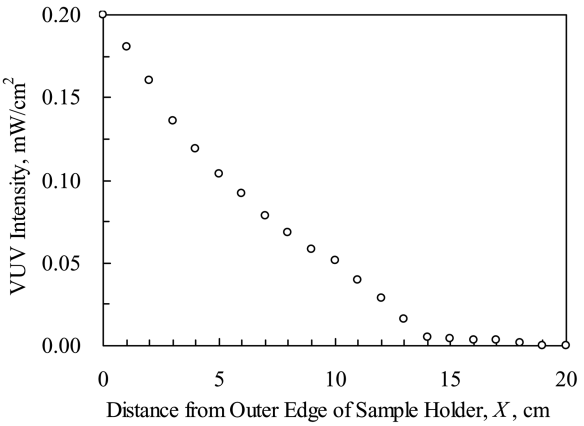

Fig. 2 VUV intensity for the distance from the outer edge of the sample holder.

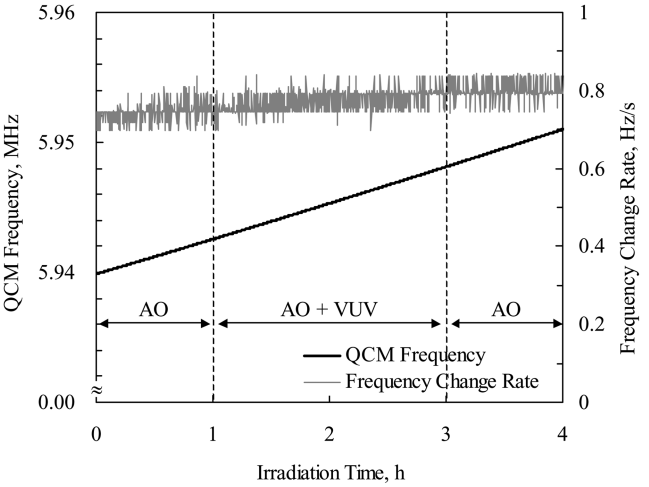

Fig. 3 QCM frequency and frequency change rate at 16 cm distance from the outer edge of the sample holder during AO and AO + VUV irradiation.

variation existed in the QCM frequency change rate at the VUV on or off points. These results indicate that the VUV intensity level at the little VUV-influenced position is sufficiently low that it does not affect the mass loss of a polyimide.

Comparison of the mass loss of the AO fluence monitor, Kapton H, between that on the sample holder and on the little VUV-influenced position showed that the ratio of Kapton H's mass loss on the sample holder to that on the little VUV-influenced position, $\Delta m_{\mathrm{msh}}/\Delta m_{\mathrm{mlvp}}$, was 2.38. Consequently, the AO fluence under simultaneous irradiation on the sample holder is calculable from the mass loss of AO fluence monitor mounted on the little VUV-influenced position through the following Eq. (3):

$$F_{\mathrm{sim}} = 2.38\Delta m_{\mathrm{mlvp}}/A_m\rho_m E_m \tag{3}$$

2. Vacuum Ultraviolet Fluence Measurement Under Simultaneous Irradiation

Figure 4 shows the VUV intensity at a wavelength of 150–170 nm on the sample holder during single VUV irradiation and simultaneous irradiation of AO and VUV. The intensity was stable in the single VUV irradiation. Then, the intensity increased approximately 0.01 mW/cm^2 by the addition of AO irradiation to VUV. After halting AO irradiation, the intensity almost reverted to the level of the previous single VUV irradiation. The increase of VUV intensity during simultaneous irradiation might result from the addition of VUV emitted in AO generation. In fact, the VUV intensity under single AO irradiation was measured as approximately 0.01 mW/cm^2, corresponding with the increased amount. Therefore, the actual VUV-source intensity on the sample holder can be determined by deducting the intensity measured in single AO irradiation from the total intensity in the simultaneous irradiation. Then, the integral intensity of VUV at a wavelength of 120–200 nm under simultaneous irradiation is calculated from the VUV spectrum, which was calibrated with the attenuations in the light path and the actual VUV-source intensity on the sample holder.

B. Synergistic Effects of Atomic Oxygen and Vacuum Ultraviolet

1. Mass and Erosion Yield

After single AO, sequential, and simultaneous irradiation, that is, *AO-inclusive* irradiation, Kapton H lost 2.5–4.0 mg of their weight; Ag-coated FEP also lost 1.2–2.2 mg of their weight after AO-inclusive irradiation. For both materials, the mass was changed little by a single VUV irradiation.

The erosion yields calculated from the mass loss are presented in Fig. 5. No obvious difference attributable to irradiation method was detected in either sample, demonstrating that the sequential or simultaneous irradiation has no effect on the erosion yield. However, Yokota et al. reported that the polyimide erosion rate under simultaneous irradiation, where VUV intensity was relatively high,

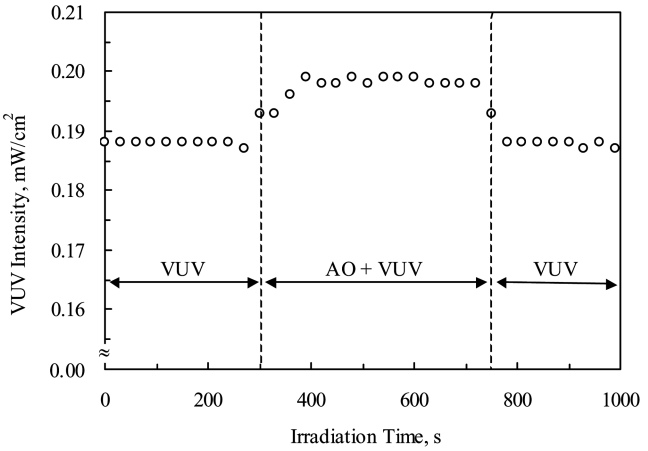

Fig. 4 VUV intensity on the sample holder during VUV and VUV + AO irradiation.

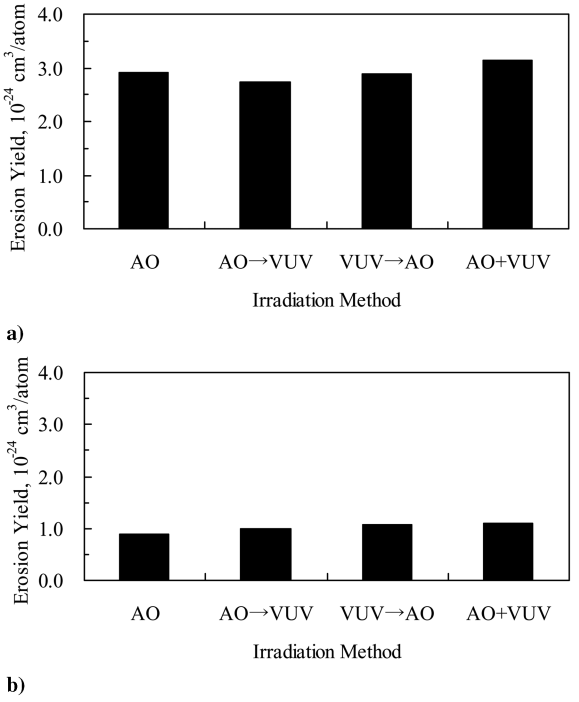

Fig. 5 Erosion yield for a) Kapton H and b) Ag-coated FEP.

was increased as high as 400% greater than the case of single AO irradiation [6]. This discrepancy is regarded to be due to the difference of the relative intensity of VUV (VUV fluence was divided by AO fluence). The VUV/AO intensity ratio in Yokota et al.'s study was 4×10^{-15}–8×10^{-15} mJ/atom, whereas, the ratio in this study was 3.7×10^{-17}–5.8×10^{-17} mJ/atom. Compared with the results of the Evaluation of Oxygen Interaction with Materials-3 experiment in LEO [11], Yokota et al. concluded that the synergistic effect on polyimide erosion surely exists, but it was not significant in the LEO environment where the relative intensity of VUV is low [6]. The fluence of AO and VUV was based on the LEO environment in our present study, thus, our results agree with their conclusion.

2. Thermo-Optical Properties

Changes of thermo-optical properties for Kapton H before and after irradiation are shown in Fig. 6. The initial thermo-optical properties of Kapton H are $\alpha_S = 0.22 \pm 0.01$ and $\varepsilon_N = 0.52 \pm 0.01$. In both α_S and ε_N, significant changes were found after AO-inclusive irradiation. The α_S was decreased slightly by VUV irradiation, but the amount of reduction was within the measurement deviation. These results reveal that AO attack is a major cause of the thermo-optical properties' changes. In general, α_S depends strongly on surface roughness. In fact, the surfaces of Kapton H irradiated by AO were changed from glossy to matte, that is, to a diffuse surface with low reflectance, thereby increasing α_S. The α_S increased similarly in each sample after AO-inclusive irradiations, suggesting that the surface roughness is equivalent in these samples and that synergistic effects are insufficient to affect the change of α_S. Moreover, the decrease in ε_N is considered to result from the thickness loss. The thinner the films become, the more infrared transmittance increases; consequently, ε_N decreases. The ε_N of the sample irradiated by AO and VUV simultaneously declined more than others, as shown in Fig. 6b, probably because the AO fluence in the simultaneous irradiation test was greater than those in other irradiation tests, leading to a higher thickness loss. Figure 7 shows that no noticeable difference exists between each sample after AO-inclusive irradiation when the ε_N changes are normalized with the thickness loss. Here, the thickness loss was calculated from the mass loss through Eq. (4):

$$\Delta t_s = \Delta m_s/A_s\rho_s \tag{4}$$

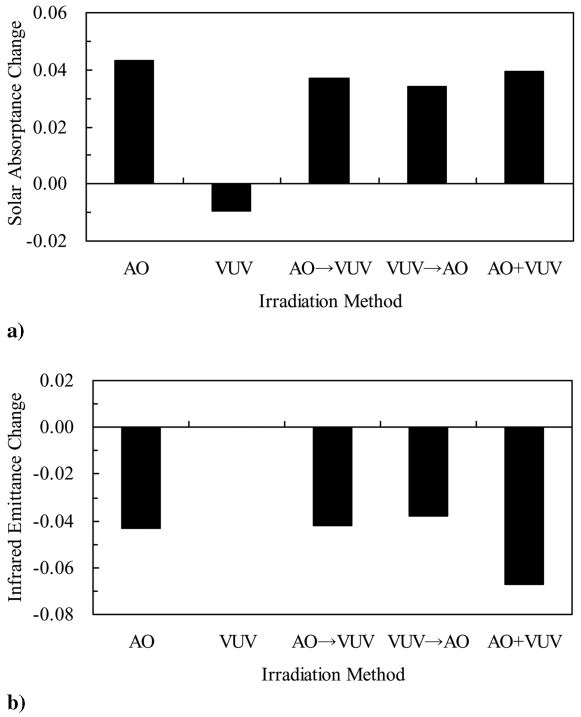

Fig. 6 Change of a) solar absorptance and b) infrared emittance for Kapton H.

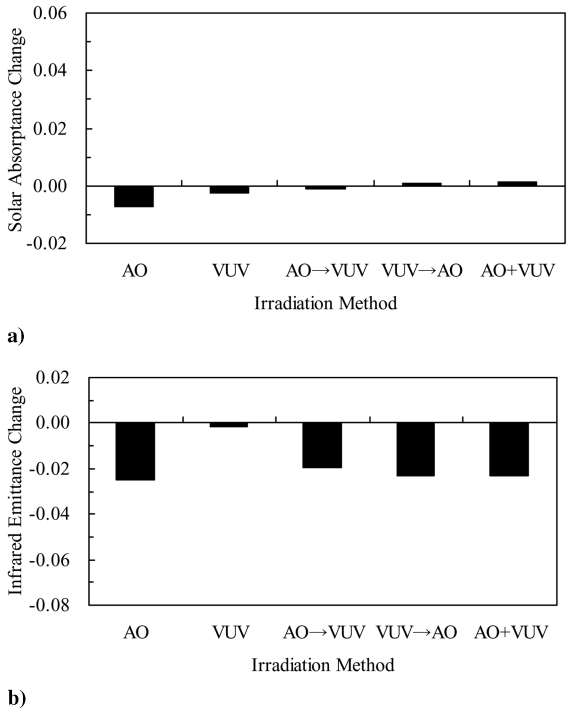

Fig. 8 Change of a) solar absorptance and b) infrared emittance for Ag-coated FEP.

Changes of the thermo-optical properties for Ag-coated FEP are shown in Fig. 8. The initial properties of Ag-coated FEP are $\alpha_S = 0.03 \pm 0.01$ and $\varepsilon_N = 0.59 \pm 0.02$. Almost no change was apparent in α_S. After AO-inclusive irradiation, the samples showed a slight decrease in the value of ε_N, but they were entirely within the measurement deviation.

3. *Surface Morphology*

As presented in Fig. 9, the Kapton H after AO-inclusive irradiation are characterized by needlelike surfaces, which is typical surface morphology of AO-irradiated polymers [1]. No major difference existed between surfaces after single AO irradiation and those after sequential or simultaneous irradiation, which agrees with the result of α_S changes.

The surface morphology of Ag-coated FEP, shown in Fig. 10, varied greatly depending on the irradiation method. The surface of pristine control samples exhibited a roughish asperity. After single AO irradiation, many sharp cones were produced on the surface, similar to the needlelike surface of AO-irradiated Kapton H. In contrast, the surface after single VUV irradiation was flatter than that of the control. In addition, the surface irradiated by VUV after AO (AO → VUV) was also smoothed. These phenomena suggest that the surface asperity was lost by VUV irradiation. Considering these results and the fact that FEP is highly sensitive to VUV [12], the convex superior positions on the surface, for example, the tops of cones, might be influenced strongly by VUV and thereby decomposed preferentially. The sample irradiated by AO after VUV (VUV → AO) exhibits a needlelike surface that is identical to that of the sample irradiated by single AO. The flat surface, which is thought to be produced by VUV irradiation, was eroded by the subsequent AO irradiation. Consequently, the surface morphology differed depending on the irradiation sequence. In simultaneous irradiation, the roughness development by AO attacks and the smoothing by VUV irradiation mutually compete. Then, a rougher surface with low blunt cones can be produced. Ag-coated FEP changed their surface morphology with irradiation method, but there was no marked difference in α_S, as shown in Fig. 8a. The surface roughness of Ag-coated FEP is too small to affect the value of α_S.

Grossman et al. also evaluated the synergetic effects of AO and VUV on surface morphology of Kapton and Teflon FEP [7,13]. According to their study, both Kapton and Teflon FEP formed rougher surfaces after the simultaneous irradiation of AO and VUV, compared with those after single AO irradiation. This phenomenon is obviously different from our current results. One of the reasons for the difference is that the VUV/AO intensity ratio in Grossman et al.'s study is higher than that in this study. In conclusion, VUV/AO intensity ratio is an important factor in evaluation for synergetic effects of AO and VUV on surface morphology.

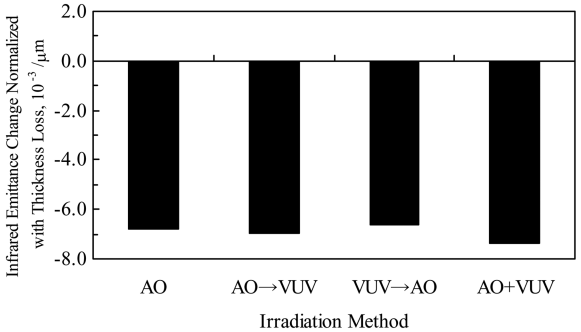

Fig. 7 Infrared emittance change normalized with the thickness loss for Kapton H.

IV. Conclusions

The measurement methods for AO and VUV fluence under simultaneous irradiation were established as follows. The little VUV-influenced positions that were sufficiently irradiated by AO and which were little affected by VUV were found. By comparing the mass loss of the AO fluence monitor, Kapton H, mounted on the sample holder with that on the little VUV-influenced position, the ratio of the Kapton H's mass loss on the sample holder to that on the little VUV-influenced position was determined. The AO fluence under simultaneous irradiation was calculated from the mass loss of AO fluence monitor mounted on the little VUV-influenced position and the mass loss ratio.

The actual VUV-source intensity on the sample holder under simultaneous irradiation was estimated by deducting the intensity measured in single AO irradiation from the total intensity measured

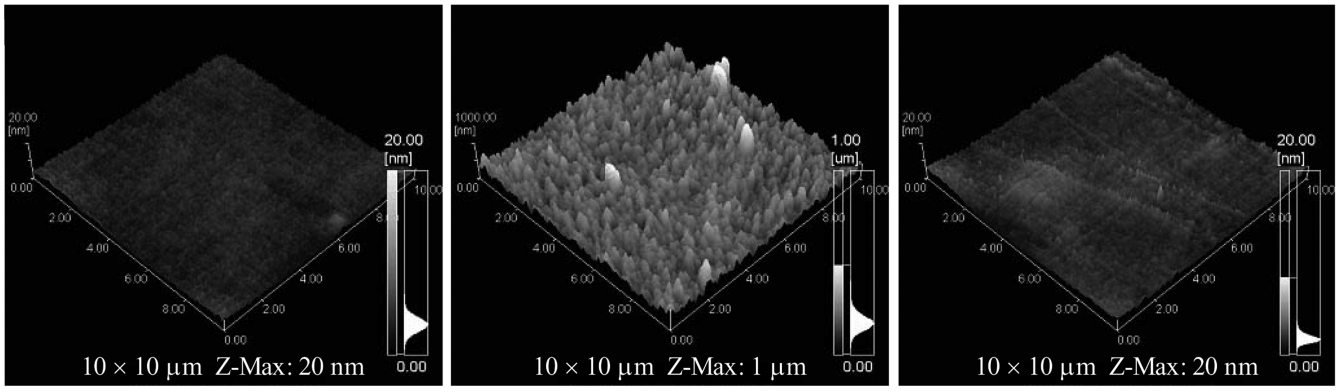

a) Control b) AO c) VUV

d) AO→VUV e) VUV→AO f) AO + VUV

Fig. 9 Surface morphology for Kapton H of a) control, and after b) AO irradiation, c) VUV irradiation, d) AO → VUV irradiation, e) VUV → AO irradiation, and f) AO + VUV irradiation.

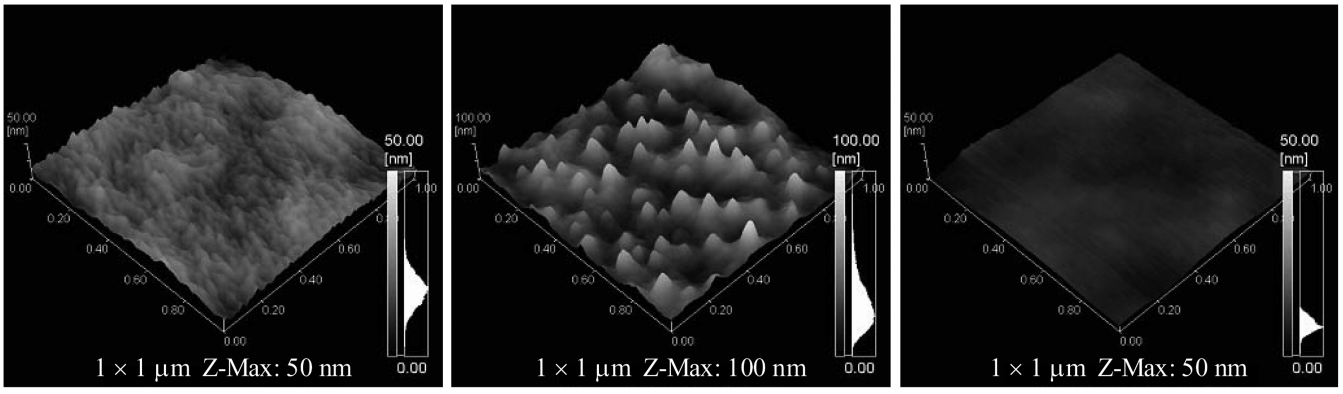

a) Control b) AO c) VUV

d) AO→VUV e) VUV→AO f) AO+VUV

Fig. 10 Surface morphology for Ag-coated FEP of a) control, and after b) AO irradiation, c) VUV irradiation, d) AO → VUV irradiation, e) VUV → AO irradiation, and f) AO + VUV irradiation.

in simultaneous irradiation. The integral intensity of VUV at a wavelength of 120–200 nm under simultaneous irradiation is calculated from the VUV spectrum, which was calibrated with the attenuations in the light path and the actual VUV-source intensity on the sample holder.

The synergistic effects of AO and VUV on Kapton H and Ag-coated FEP were investigated using single, sequential, and simultaneous irradiations, where both AO and VUV fluence were equivalent to the LEO environment at around 400 km altitude for 3 months. Results showed no obvious difference in erosion yields attributable to irradiation method for either material. Thermo-optical properties of Kapton H were degraded by AO-inclusive irradiations, and the degradation levels were similar in each sample. The Ag-coated FEP underwent no marked changes in thermo-optical properties after each irradiation. These results indicate that the synergistic effects of AO and VUV have no influence on the erosion yield and thermo-optical properties for either material under the experimental conditions used in this study. Kapton H samples exhibited needlelike surfaces after AO-inclusive irradiation; the VUV irradiation had no effect on the Kapton H surface morphology. For Ag-coated FEP, the surface irradiated by AO was also characterized by a needlelike surface. The surface of Ag-coated FEP irradiated by VUV become flatter than the original, which suggests that VUV might have an effect of smoothing Ag-coated FEP surfaces. After sequential irradiation, the surface morphology differed depending on the irradiation sequence. A rougher surface with low blunt cones was produced by simultaneous irradiation resulting from the interaction between the erosion by AO attacks and smoothing by VUV irradiation.

Acknowledgments

The authors gratefully acknowledge the experimental support of Susumu Baba, Kensuke Takahashi, Kaori Umeda, and Yuka Iizuka (Advanced Engineering Services).

References

[1] Tennyson, R. C., "Atomic Oxygen and Its Effects on Materials," *The Behavior of Systems in the Space Environment*, edited by R. N. DeWitt, Kluwer Academic, Norwell, MA, 1993, pp. 233–357.

[2] Shimamura, H., and Yamagata, I., "Degradation of Tension-Loaded Polyimide Films in a Space Environment: Results of the SM/MPAC&SEED Mission," *Proceedings of the 10th International Symposium on Materials in a Space Environment and the 8th International Conference on Protection of Materials and Structures in a Space Environment* [CD-ROM], ESA Publ., Noordwijk, The Netherlands, 2006.

[3] Miyazaki, E., and Shimamura, H., "Investigations into Ground Simulations Tests Used to Evaluate Synergistic Effects on Materials," *Proceedings of the 10th International Symposium on Materials in a Space Environment and the 8th International Conference on Protection of Materials and Structures in a Space Environment* [CD-ROM], ESA Publ., Noordwijk, The Netherlands, 2006.

[4] Marco, J., and Remaury, S., "Evaluation of Thermal Control Coatings Degradation in Simulated Geo-Space Environment," *High Performance Polymers*, Vol. 16, No. 2, 2004, pp. 177–196. doi:10.1177/0954008304044102

[5] Nakayama, Y., Imagawa, K., Tagashira, M., Nakai, M., Kudoh, H., Sugimoto, M., Kasai, N., and Seguchi, T., "Evaluation and Analysis of Thermal Control Materials Under Ground Simulation Test for Space Environment Effects," *High Performance Polymers*, Vol. 13, No. 3, 2001, pp. S433–S451. doi:10.1088/0954-0083/13/3/334

[6] Yokota, K., Ohmae, N., and Tagawa, M., "Effect of Relative Intensity of 5 eV Atomic Oxygen and 172 nm Vacuum Ultraviolet in the Synergism of Polyimide Erosion," *High Performance Polymers*, Vol. 16, No. 2, 2004, pp. 221–234. doi:10.1177/0954008304044123

[7] Grossman, E., Gouzman, I., Lempert, G., Noter, Y., and Lifshitz, Y., "Assessment of Atomic-Oxygen Flux in Low-Earth-Orbit Ground Simulation Facilities," *Journal of Spacecraft and Rockets*, Vol. 41, No. 3, 2004, pp. 356–359. doi:10.2514/1.10890

[8] Tanaka, Y., Iwaki, M., Obara, S., and Nagata, H., "New High Vacuum Test Facilities for Mechanical Components (Pt. 1): UHV Surface Properties Test Facility and Combined Space Effects Test Facility," *Proceedings of 21st International Symposium on Space Technology and Science*, Japan Society for Aeronautical and Space Science No. 98-e-21, 1998.

[9] Oyama, K.-I., Suzuki, K., Kawashima, N., Zalpuri, K. S., Teii, S., and Nakamura, Y., "An Extreme Ultraviolet Radiation Source for the Simulation of Ionosphere," *Review of Scientific Instruments*, Vol. 62, No. 7, 1991, pp. 1721–1726. doi:10.1063/1.1142412

[10] Weihs, B., and Van Eesbeek, M., "Secondary VUV Erosion Effects on Polymers in the ATOX Atomic Oxygen Exposure Facility," *Proceedings of the 6th International Symposium on Materials in a Space Environment*, European Space Research and Technology Center, Noordwijk, The Netherlands, 1994, pp. 277–283.

[11] Brinza, D. E., Chung, S. Y., Minton, T. K., and Liang, R. H., "Final Report on the NASA/JPL Evaluation of Oxygen Interactions with Materials-3 (EOIM-3)," Jet Propulsion Lab. Publ. 94-31, 1994.

[12] George, G. A., Hill, D. J. T., O'Donnell, J. H., Pomery, P. J., and Rasoul, F. A., "A Study of the UV and VUV Degradation of FEP," NASA CP 3194, Pt. 3, 1992, pp. 867–876.

[13] Grossman, E., Noter, Y., and Lifshitz, Y., "Oxygen and VUV Irradiation of Polymers: Atomic Force Microscopy (AFM) and Complementary Studies," *Proceedings of the 7th International Symposium on Materials in a Space Environment*, ONERA, Toulouse, France, 1997, pp. 217–223.

J. Minow
Associate Editor